Journal of Materials Chemistry

Cite this: *J. Mater. Chem.*, 2011, **21**, 7130

www.rsc.org/materials

PAPER

pH-controllable release using functionalized mesoporous silica nanoparticles as an oral drug delivery system†

Shih-Hsun Cheng, Wei-Neng Liao, Li-Ming Chen and Chia-Hung Lee*

Received 22nd December 2010, Accepted 16th March 2011
DOI: 10.1039/c0jm04490c

We designed a novel oral colon-specific drug delivery system (OCDDS) using a modification of mesoporous silica nanoparticle (MSN) surfaces with pH-sensitive trimethylammonium (TA) groups through a pH-sensitive hydrazone bond. The pH-sensitive TA groups can efficiently increase the loading amounts of anionic drugs by a strong electrostatic attraction. After oral administration, the acidic pH of gastric juice can fully hydrolyze the TA–hydrazone bonds and further eliminate the positive charges of TA groups from MSN surfaces. When the hydrolyzed complexes were further delivered to the colon's pH of 7–8, a rapid and complete release of adsorbed drugs was observed. From the studies of spectroscopic characterizations, we demonstrated that the combination of pH-sensitive hydrazone–TA groups and nano-sized particles of the MSN carriers took the advantages of increasing the accessible surface areas of drug molecules and varying the charges of MSN surfaces, which can increase dissolution and release rate of hydrophobic drug molecules. In addition, a cell viability assay also indicated that no cytotoxicity of MSN–hydrazone–TA complexes was observed even with treatment in an extremely high nanoparticle concentration. Consequently, our new formulation is highly biocompatible for the OCDDS, and we can completely solve the low stability, low solubility, and low drug bioavailability in the free form of drug molecules for the design of OCDDS.

Introduction

With the progress of human civilization, dietary habits have become diversified; therefore, many gastrointestinal diseases such as inflammatory bowel disease and gastrointestinal cancer have grown progressively in recent years. The use of oral administration is the first priority for delivering drug molecules for colon-related diseases such as irritable bowel syndrome, Crohn's disease, ulcerative colitis, and colon cancer. For the purpose of pharmacotherapy, the delivery of drug molecules through the oral route can provide patient compliance, convenience, and increase the therapeutic efficacy. Especially, the design of an oral colon-specific drug delivery system (OCDDS) has the advantage of being more effectively treated when the therapeutic drugs are delivered to the colon tissue.[1] To increase the drug bioavailability, the design of an OCDDS should be formulated to protect the fragile drug molecules to overcome the dissociation by the enzymes (for example, pepsin) and the low pH of gastric acid in the stomach. The major OCDDSs developed during the past decade are based on the formulation of time-controlled release, pH-sensitive coated tablets, and colon-specific prodrug systems. Time-controlled release is designed to regulate the dissolution rate of the coated polymers, which can delay the onset of drug release until the formulated drugs have reached the colon tissues.[2–6] The pH-sensitive coated tablets are based on the solubility of the coated pH-sensitive polymers at various pH values of the GI tract, which increases from the stomach (pH 1.0–3.0) to the small intestine (pH 6.5–7.0), and to the colon (pH 7.0–8.0).[7–10] When the formulated drugs pass through the low pH of stomach fluid, the low solubility of enteric coating shells can efficiently protect the drug core from dissociation. Furthermore, the high pH values of the colon can accelerate the release of the drug core through the increasing solubility of the coated shells. For the prodrug strategy, the prodrug molecules can be activated by a bacteria-catalyzed reaction in the colon (approximately 10^{12} CFU mL^{-1}).[11] The major metabolic enzymes, such as reducing and hydrolytic enzymes in the colon-bacteria, can activate the prodrug molecules through the hydrolysis of ester/amide bonds or the reduction of azo-bonds.[12] Although many researchers have studied OCDDSs through the above three approaches, the increase of drug bioavailability in OCDDSs still encounters numerous challenges.[13–16]

In recent years, mesoporous silica materials have inspired considerable interest for use as the novel drug delivery system.[17–24] Due to the large surface area, large pore volume, highly ordered pore structure, and adjustable pore size, mesoporous silica material can load and protect therapeutic drugs and further

Department of Life Science and Institute of Biotechnology, National Dong Hwa University, Hualien, 974, Taiwan. E-mail: chlee016@mail.ndhu.edu.tw; Fax: +886-3-863-3630; Tel: +886-3-863-3682

† Electronic supplementary information (ESI) available: Thermo-gravimetric analyses (TGA) of various samples of weight loss (Fig. S1) and *ex vivo* fluorescence imaging of excrement and organs (Fig. S2). See DOI: 10.1039/c0jm04490c

control the release of pre-loaded drug molecules.[25] Several research groups have studied the sustained-release properties of drugs loaded in conventional mesoporous silica microsized particles (that is, MCM-41, MCM-48, and SBA-15).[26–29] Vallet-Regi *et al.* proposed these versatile hosts as implantable, oral, transdermal, injectable drug reservoirs, and for bone tissue regeneration.[30–35] Previous studies have indicated that the drug molecules can adsorb inside the non-functionalized silica matrix through a weak attraction (that is, hydrogen bonding) which usually causes a low loading capacity.[36] To increase the loading amounts of drug molecules, the silica surfaces can modify with ionic charges or hydrophobic groups, which can produce a strong electrostatic attraction or π–π interaction with the drug molecules.[37–39] Furthermore, the release mechanism was triggered through the increase of physiologically ionic strength, electrostatic repulsion, light irradiation, pH variation, temperature regulation, perturbed magnetic field, and chemical or enzymatic degradation.[40–53] In various approaches for drug loading and releasing mechanisms, the use of electrostatic attractions and the pH dependent release has been extensively applied and studied for oral drug delivery systems.[42] Owing to the drug storage capacity and release efficacy related to surface properties of the drug carriers, the modified density of functional groups in the drug carriers and the drug concentrations (or the pH value) of the adsorbed solution were all important.[37] Although the increase of positive-charged functional groups on the surfaces of the drug carriers can increase the loading amounts of an anionic drug, the strong electrostatic attractions restrain the releasing rate of free drug molecules when the formulated drugs are delivered to the targeted site. The low releasing rate usually caused the delayed release of drug molecules, which may still remain in their carriers to excrete into the feces. Therefore, a low drug bioavailability is observed. For this reason, we propose a new strategy for pH-responsive mesoporous silica nanoparticles (MSNs) to control release of an anionic drug for the OCDDS. Ritter *et al.* have reported that the behavior of the functionalized MSN through post-modification is substantially different from the corresponding microparticles. Due to the short channel lengths of MSN, the total surface areas are the major contribution from the external surfaces.[54,55] For a drug nanoparticle to dissolve in a liquid medium, the dissolution velocity (dC_x/dt) increases with decreasing the particle size. The Noyes–Whitney equation (1) explains that the increase of the exposed surface areas to the dissolved medium can increase the dissolution velocity of the drug molecules. However, the decrease in the thickness of diffusible layer (h) can efficiently accelerate the dissolution velocity.[56]

$$dC_x/dt = DA(C_s - C_x)/h \quad (1)$$

The use of MSN as the drug carrier can increase the dissolution velocity through: (a) the increase of contact surfaces of the drug molecules and the physiological buffer and (b) the decrease in the thickness of diffusible layer by monolayer adsorption of the drug molecules in the MSN surfaces; therefore, an increase of bioavailability of a hydrophobic drug can easily be achieved. Because of the shield effect of drug molecules in the surfaces of MSN, we modified the trimethylammonium (TA) groups on MSN through a pH-sensitive hydrazone bond and, thus, a highly positive charge of TA groups generated a strong electrostatic attraction for high loading of anionic drugs. Furthermore, the hydrolysis of most hydrazone bonds in the stomach pH produced a strong electrostatic repulsion, which triggered the rapid release of adsorbed drug molecules.

Experimental section

Materials

Tetraethoxysilane (TEOS), cetyltrimethylammonium bromide (CTAB), ethanol, ammonium hydroxide (30%), $NaH_2PO_4 \cdot H_2O$, Na_2HPO_4, DMSO, and HCl (37%) were purchased from Acros. The *n*-octane was purchased from Alfa Aesar. Sulfasalazine, acethydrazide trimethylammonium, and 3-(4,5-dimethylthiazol-2-yl)-2,5-diphenyltetrazolium bromide (MTT) were purchased from Sigma. Triethoxysilylbutyraldehyde was obtained from Gelest. A RPMI-1640 medium, fetal bovine serum, penicillin, and streptomycin were obtained from GIBCO/BRL Life Technologies (Grand Island, NY, USA).

Preparation of MSN

Large pore diameters of MSN samples, with hexagonal well-ordered pore structures, were synthesized in a low concentration TEOS, a surfactant (CTAB), and a base catalyst (NH_4OH), in a two-step preparation. The sol–gel process, for the co-condensation of TEOS to synthesize MSNs, was as follows. First, CTAB (0.58 g) was dissolved in NH_4OH (0.51 M, 300 mL) at 40 °C and 5.0 g of the structural swelling agent (*n*-octane) was then added. After stirring for 1 h, 5 mL of 0.2 M TEOS (in ethanol) was added with vigorous stirring. After the solution was further stirred for 5 h, 5 mL of 1.0 M TEOS (in ethanol) was added with vigorous stirring for another 1 h. The solution was aged at 40 °C for 20 h. Samples were collected by centrifuging at 12 000 rpm for 20 min, washed, and redispersed in deionized water and ethanol several times. The solid products were obtained by centrifugation. The surfactant templates were removed by extraction in acidic ethanol (approximately 1.0 g of HCl in 50 mL of ethanol at 65 °C for 24 h).[57]

Synthesis of aldehyde-modified MSN

The anchoring of aldehyde–silane groups onto the surfaces of MSN was accomplished as follows. First, 200 mg of the extracted MSN was placed in 50 mL of toluene and stirred for 30 min. Then, 800 μL of triethoxysilylbutyraldehyde was then added to the resulting suspension and allowed to react for 20 h at 80 °C. Samples were collected by centrifuging at 12 000 rpm for 20 min, washed, and redispersed in acetone several times.

Conjugation of acethydrazide trimethylammonium in aldehyde-modified MSN

Conjugation of acethydrazide trimethylammonium groups on MSN surfaces was achieved through the nucleophilic addition of aldehyde-modified MSN and acethydrazide trimethylammonium to produce a hydrazone bond. The reaction conditions were as follows. First, 200 mg of aldehyde-modified MSN was suspended in 10 mL of anhydrous methanol. Next, 200 mg of

acethydrazide trimethylammonium was added to the above solution, followed by two drops of acetic acid. The solution was then stirred at room temperature for 24 h. The solids of MSN–hydrazone–TA samples were isolated by centrifuging at 12 000 rpm for 20 min, washed, and redispersed in methanol several times.

Preparation of the sulfasalazine-loaded MSN–hydrazone–TA samples

To prevent the hydrolysis of pH-sensitive linker and increase the solubility and loading percentages of sulfasalazine, we used DMSO as the solvent to load sulfasalazine in the MSN carriers. The experimental steps were as follows. First, 20 mg of MSN–hydrazone–TA samples were added to 1.5 mL (10 mM) of sulfasalazine. The mixture was stirred at 800 rpm for 4 h. At the end, the particles were washed with DMSO, centrifuged at 12 000 rpm for 20 min and further dried under vacuum. The residual solution was analyzed with a UV-Vis spectrometer. Sulfasalazine adsorbed in the nanoparticles was determined by measuring the decrease of absorption peak at 360 nm.

In vitro release study

In vitro release experiments were performed in simulated gastrointestinal fluids (pH 1.2 of 0.1 M HCl; pH 5.0, 7.4, and 8.0 of 0.1 M Na_2HPO_4–NaH_2PO_4 buffer) to mimic sulfasalazine release in the stomach, duodenum, small intestine, and colon. The experimental condition was as follows. First, 4 mg of sulfasalazine-adsorbed MSN–hydrazone–TA samples was added into 1 mL of 0.1 M HCl (pH 1.2) and maintained at 37 °C for 4 h with shaking at 150 rpm to mimic the gastric emptying time. Then, we changed the pH values of the incubated solution to 5.0, 7.4, and 8.0 to study the release rate of sulfasalazine in the duodenum, small intestine, and colon. The release medium was removed for analysis at given time intervals by centrifuging at 12 000 rpm for 20 min. The residual solids were added to the same volume of fresh simulated fluids. The released percentage of the sulfasalazine in the solution phase was determined by measuring the increase of absorption peak at 360 nm at the constant pH (9.0).

Cell culture

HT-29 (human colon cell line) was cultured in an RPMI-1640 medium supplemented with 10% (v/v) fetal bovine serum and penicillin (100 units mL^{-1})/streptomycin (100 μg mL^{-1}). Cultures were maintained in a humidified incubator at 37 °C in 5% CO_2.

Cell viability assay

MTT assay was used to measure the effects of MSN–hydrazone–TA on cell viability. Cells were inoculated into 96-well plates at the density of 10 000 cells per well. After 24 h for the cell attachment, cells were treated with various concentrations (1, 2, 10, 20, 100, 200, 250, and 500 μg mL^{-1}) of the MSN–hydrazone–TA sample and incubated for another 24 h. At the end of incubation, we added 100 μL of MTT solution (1 mg of MTT in 1 mL of PBS) and further incubated at 37 °C for 4 h. Finally, we pirated the medium and dissolved the violet crystals (formazan) with 150 μL of DMSO, and the reduction of MTT by mitochondrial dehydrogenase was measured at 550 nm using an ELISA reader. Cells without added nanoparticles were taken as the control experiment and the viability was set as 100%.

Characterization

The surface area, pore size, and pore volume were determined by N_2 adsorption–desorption isotherms obtained at 77 K on a Micrometric ASAP 2020 apparatus. The sample was outgassed at 10^{-3} Torr and 120 °C for approximately 6 h prior to the adsorption experiment. The pore size distribution curves were obtained from the analysis of the adsorption portion of the isotherms using the BJH (Barrett–Joyner–Halenda) method. UV-visible spectra were taken with a GeneQuant 1300 (GE Healthcare) spectrophotometer. The spectra were collected at the intensity of 360 nm wavelength for sulfasalazine against a standard. FT-IR spectra were recorded on a Nicolet 550 spectrometer with a KBr pellet. Approximately 1 mg of a sample was mixed with 300 mg of dried KBr and then pressed. The ζ-potentials of various MSN samples were measured in a Malvern Nano-HT Zetasizer. The ζ-potential distribution was obtained by an average of ten measurements. The samples were prepared at a concentration of 2 mg in 1 mL of dd-H_2O. The ζ-potential from different pH values (2–9) was measured by an auto-titration system.

Results and discussion

As shown in Fig. 1, the synthesis of hydrazone-conjugated TA groups on the surface of MSN was achieved through the reaction

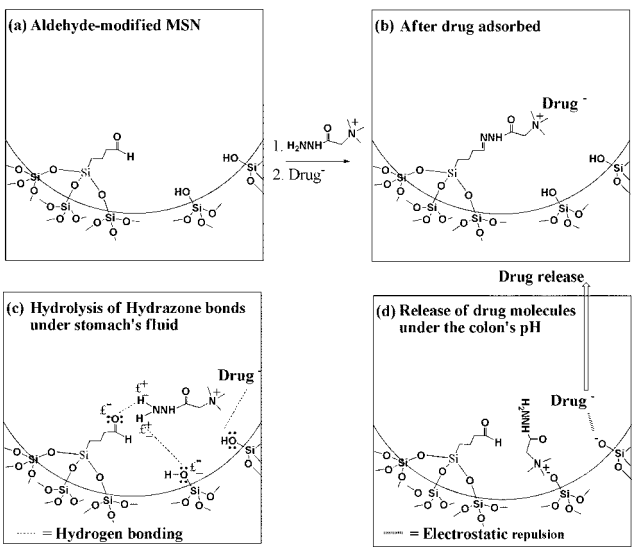

Fig. 1 The representation of the pH dependent release system of an anionic drug (sulfasalazine) adsorbed in MSN samples through a pH-sensitive TA group. (a) Aldehyde-modified MSN surfaces, (b) the synthesis of pH-sensitive MSN–TA by a hydrazone bond and the further adsorbent drug molecules by electrostatic attractions, (c) drug adsorbed and protected in the nanochannels of MSN by the help of hydrogen bonding in the stomach's acidic environment, and (d) the burst release of the adsorbed drug molecules by electrostatic repulsion in the neutral pH of the intestinal fluid.

of TA–hydrazide groups with the aldehyde-modified MSN (Fig. 1a). The modification of TA-groups on the MSN surfaces can increase the positive charges of MSN; therefore, the negative charge of drug molecules has high loading in the TA-modified MSN through strong electrostatic attractions. When the MSN stayed in the stomach pH, the hydrazone bonds all demonstrated hydrolysis, but the drug molecules were temporally entrapped in the nanochannels of MSN through hydrogen bonding of various functional groups. Then the adsorbed drugs produced a strong repulsion when the pH of the solution rose to 7–8 of the colon pH. The mechanism for the burst release of drug molecules in the colon pH may come from the extinction of the positive charged TA through the formation of an ion pair with the deprotonated silanol groups on MSN surfaces. Furthermore, the production of many deprotonated silanol groups (SiO^- groups) can generate a strong electrostatic repulsion, which can achieve the burst release of anionic drug molecules in the colon pH. To demonstrate this strategy, we loaded a negative charge of the commercially available anti-inflammatory prodrug (sulfasalazine) in the nanochannels of MSN–hydrazone–TA. After the release of sulfasalazine from the nanochannels of MSN, the sulfasalazine can be activated through the reduction and cleavage of the azo-bond by colonic bacteria (azoreductases) *in vivo* and, therefore, produce 5-aminosalicylic acid (5-ASA), which acts as an active moiety in the treatment of two major human chronic inflammatory bowel diseases (Crohn's disease and ulcerative colitis).[12] Our studies showed that the hydrolysis of most hydrazone bonds could be achieved in 4 h. The time for hydrolysis periods was matched with the gastric emptying time so we could efficiently eliminate the electrostatic attractions from TA groups, once the formulated drugs were delivered into the intestinal fluid. This new pH-triggered release mechanism combined the advantages of time-controlled release, pH-sensitive delivery, and prodrug strategies for rapid and complete release of pre-loaded drugs. Moreover, the nanoparticle form of mesoporous silica has large surface areas; therefore, the incorporation of drug molecules on MSN surfaces can efficiently increase the accessible surface areas between the drug molecules and the physiological buffer. Thus, the nanoparticle formulation can efficiently improve the drug bioavailability through increasing the dissolution rate of free drug molecules when they are delivered to the colon-targeted site.[8] The silica-based materials are also acid resistant, which can protect drug molecules in the stomach pH; hence, MSN is a suitable carrier for an oral drug delivery system. The MSN modified with pH-sensitive TA groups could demonstrate their potential applications for high drug-loading capacity and high efficient release, which can contribute to the pharmaceutical industry by developing OCDDSs.

To conjugate the pH-sensitive TA ligands and further load with sulfasalazine into the nanochannels of MSN, we synthesized large-pore MSN samples (about 5.0 nm). The hexagonal well-ordered pore structure was synthesized through sol–gel co-condensation of tetraethoxysilane (TEOS) in the presence of a surfactant (CTAB), a swelling agent (*n*-octane), and a base catalyst (NH_4OH). After extraction of the as-synthesized MSN by HCl/alcohol solution, the MSN surfaces were further modified with aldehyde groups by adding triethoxysilylbutyraldehyde under the reflux temperature of toluene. Next, the aldehyde-modified MSN reacted with acethydrazide trimethylammonium to produce a pH-sensitive TA group through hydrazone bonds. Nitrogen adsorption–desorption isotherms and pore-size distributions of MSN, MSN–aldehyde, MSN–hydrazone–TA, and MSN–hydrazone–TA–sulfasalazine samples are shown in Fig. 2.

The surface areas are gradually decreased from 1265 $m^2\ g^{-1}$ of MSN to 823 $m^2\ g^{-1}$ of MSN–aldehyde, to 634 $m^2\ g^{-1}$ of MSN–hydrazone–TA, and to 520 $m^2\ g^{-1}$ of the sulfasalazine-adsorbed MSN–hydrazone–TA sample. Simultaneously, the pore volumes and pore diameter decreased from 1.675 $cm^3\ g^{-1}$ and 5.2 nm for MSN to 0.935 $cm^3\ g^{-1}$ and 4.7 nm for MSN–aldehyde, to 0.651 $cm^3\ g^{-1}$ and 4.1 nm for MSN–hydrazone–TA and to 0.502 $cm^3\ g^{-1}$ and 3.2 nm for the sulfasalazine-adsorbed MSN–hydrazone–TA sample.

Thus, the modification of the aldehyde groups, the further conjugation of the TA–hydrazide linker, and the final adsorption of the sulfasalazine molecules can easily be observed by the reduction of the three parameters. TEM images of MSN–hydrazone–TA (Fig. 3) show that the sample generally has a round shape and a uniform size, with average particle diameters of approximately 50 nm. Using *n*-octane as a swelling agent to expand the inner micelle space, the as-synthesized MSN possessed both large pore diameters (*ca.* 5.0 nm) and well-ordered pore structures. Moreover, the MSN morphology and the structure were not affected by the conjugation and loading of the TA–hydrazide linkers and drug molecules onto the MSN surface.

To characterize the chemical bonds and surface organic groups within our MSN samples and their post-synthesis modifications and conjugations, we employed FT-IR spectroscopy. The FT-IR spectra of bare MSN (Fig. 4a) reflect only the surface silanol groups and low frequency silica vibrations. The C–H stretches at 2940 cm^{-1} and 2980 cm^{-1} appear only on surface functionalized MSN samples (Fig. 4b and c). The aldehyde-modified MSN sample displays C═O stretch modes at or near 1715 cm^{-1} (Fig. 4b). Conjugation of acethydrazide trimethylammonium groups in MSN–aldehyde surfaces produced TA

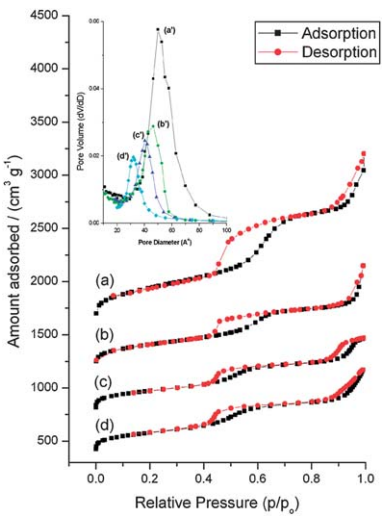

Fig. 2 Nitrogen adsorption–desorption isotherms of (a) MSN, (b) MSN–aldehyde, (c) MSN–hydrazone–TA, and (d) sulfasalazine adsorbed on MSN–hydrazone–TA samples. Corresponding pore size distributions (inset: a′, b′, c′, and d′).

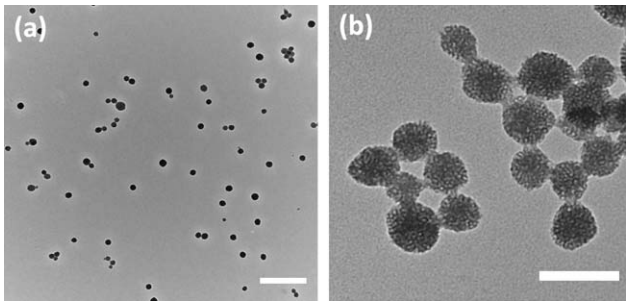

Fig. 3 TEM images of the characteristic hexagonal structure of MSN–hydrazone–TA. Scale bars: (a) 500 nm and (b) 100 nm.

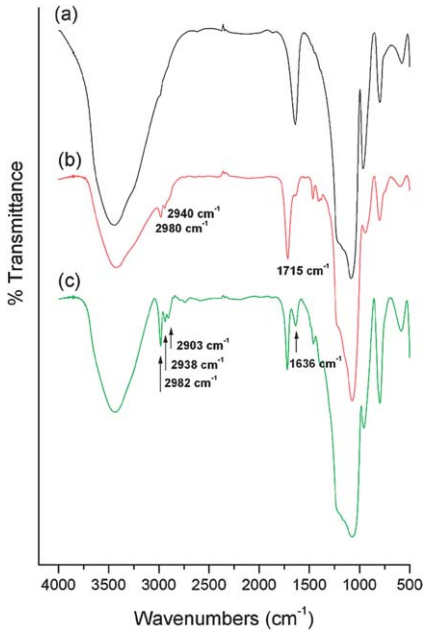

Fig. 4 FT-IR spectra of (a) the MSN after extraction in a HCl–EtOH solution, (b) the MSN modified with aldehyde groups, and (c) the MSN–aldehyde sample modified with TA groups through the formation of a hydrazone bond.

groups with a hydrazone bond, as seen in the absorption peaks of imine (C═N) at 1636 cm^{-1}. Other bands at 1400 cm^{-1} are attributed to CH_2 bends. Especially, the TA-modified MSN surfaces showed strong C–H stretching bands at 2903, 2938, and 2982 cm^{-1} (from trimethyl groups), which indicated that the TA groups exhibited high loading in the MSN surfaces.[58]

We also measured the ζ-potential of MSN–hydrazone–TA before (Fig. 5b) and after hydrolysis (Fig. 5c) in the stomach pH (1.2) for 4 h. For ζ-potential measurements, the samples in dd-H_2O were titrated with the pH ranging from 2 to 9 automatically. Due to the positive charges of the TA groups, the MSN–hydrazone–TA sample showed highly positive ζ-potential value (approximately +38 mV) within the pH range of 3 to 6. The pH value of point zero charge (PZC) for the MSN–hydrazone–TA sample was 7.38. After the hydrolysis of MSN–hydrazone–TA sample at pH 1.2 for 4 h, we washed the sample surfaces with dd-H_2O to remove the hydrolyzed TA groups. We can observe that the titrated curve of the hydrolyzed MSN–hydrazone–TA sample (Fig. 5c) was nearly matched with the aldehyde-modified

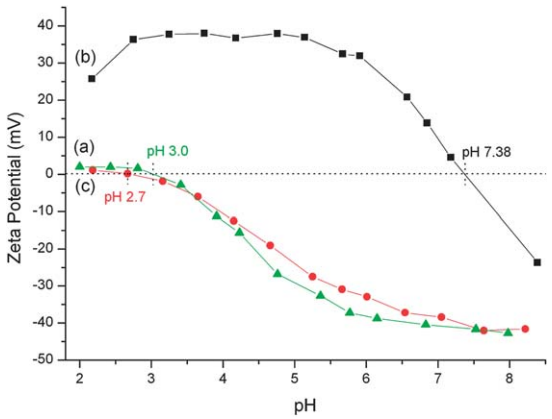

Fig. 5 ζ-Potential of (a) aldehyde-modified MSN, (b) MSN–hydrazone–TA, and (c) after hydrolysis of MSN–hydrazone–TA in pH 1.2 for 4 h.

MSN sample (Fig. 5a). The pH values of PZC in MSN–aldehyde and the hydrolyzed MSN–hydrazone–TA samples were 3.0 and 2.7, respectively. From the above results of ζ-potentials, we can infer that the most TA groups of the MSN–hydrazone–TA sample were hydrolyzed in pH 1.2 for 4 h. In addition, the ζ-potential of the hydrolyzed MSN–hydrazone–TA sample was −41 mV at pH 7.4, and, therefore, a high electrostatic repulsion from the negative silica surfaces (deprotonated silanol) and the anionic drug molecules were produced to promote the burst release of adsorbed drug molecules.

To increase the sulfasalazine solubility, we used DMSO as a dissolved solvent to increase loading amounts of hydrophobic drug molecules. Sulfasalazine was loaded into MSN–hydrazone–TA at room temperature and the loading amounts were also confirmed by the absorption decrease of UV-Vis at 360 nm. The maximum adsorption of MSN–hydrazone–TA samples in the sulfasalazine/DMSO solution was 168.5 μmol g^{-1}. In addition, the thermogravimetric analyses (TGA) profiles of weight loss are summarized in Fig. S1, ESI†.

The decomposition of MSN complexes by the heating process comes mainly from the loss of adsorbed H_2O from MSN surfaces and further from the combustion of organic ligands and adsorbed drugs. The TGA profiles of MSN only, aldehyde-modified MSN, conjugation of TA–hydrazide groups, and the further loading of sulfasalazine showed a weight loss of 5.61% (Fig.-S1a†), 20.83% (Fig. S1b†), 25.08% (Fig. S1c†) and 32.89% (Fig. S1d†), respectively. From the TGA data, we may estimate that the weight percentage of sulfasalazine in MSN–hydrazone–TA–sulfasalazine was 7.8%. This weight loss percentage of sulfasalazine is extremely close to our quantitative results from UV-Vis absorption (wt% = 6.7). The release profiles of loaded sulfasalazine molecules at the MSN–hydrazone–TA samples were studied in the simulated gastrointestinal fluids of various pH values (1.2, 5.0, 7.4, and 8.0 corresponding to the stomach, duodenum, small intestine, and colon pH). All the MSN–hydrazone–TA–sulfasalazine samples were initially incubated in a simulated gastric fluid (pH 1.2) for 4 h to mimic the gastric emptying time, and the drug nanoparticles were then dispersed into the simulated solution at pH 1.2, 5.0, 7.4, and 8.0. To determine the charges of sulfasalazine molecules and silica surfaces at a given pH, we calculated the degree of ionization of

the carboxylic acid and silanol groups by the Henderson–Hasselbalch equation (2), which is shown below.[59]

$$\mathrm{pH} = \mathrm{p}K_a + \log \frac{[\mathrm{A}^-]}{[\mathrm{HA}]} \quad (2)$$

The pK_a value of the carboxylic acid and the silanol group in the sulfasalazine molecule and the MSN surface was 2.4 and 3.5, respectively. Therefore, the calculations of the [A^-] percentages from the carboxylic acid and the silanol group of the deprotonated forms were 6.0% and 0.5% at pH 1.2 and near 100% of the deprotonated form at the pH of 7.4 and 8.0. The ratios of [A^-] to [HA] indicated that most sulfasalazine molecules and silanol groups were shown to be un-charged forms at pH 1.2. However, nearly 100% of sulfasalazine molecules and silanol groups were de-protonated and showed negative charges when the pH values rose to 7.4 and 8.0. The release profiles are shown in Fig. 6.

The MSN–hydrazone–TA–sulfasalazine samples were observed with a lowest initial release of 15% at pH 1.2 at 37 °C for 4 h. Further we still kept the pH value in 1.2, the sulfasalazine was shown 54% slow released until 17 h. However, we changed the pH value of incubated solution to 5.0, 7.4, and 8.0, respectively. In another 4 h, we observed the burst release of 80% at pH 7.4 and 8.0. The burst release is different compared to the sustained release property using the TA-modified MSN to adsorb sulfasalazine without the help of a pH-sensitive hydrazone bond. We suggested the release of sulfasalazine molecules from MSN–hydrazone–TA samples dependent on electrostatic repulsions (Fig. 1d). While the samples were submerged in the acidic environment, the hydrazone bonds demonstrated rapid hydrolysis. However, the drug molecules and MSN surfaces were uncharged and entrapped in the nanochannels by hydrogen bonding (Fig. 1c). At the colon pH (7–8), the silanol groups (Si–OH) on the MSN surface would become de-protonated (−40 mV). Then a strong electrostatic repulsion from the negative charges of MSN (from SiO^- groups) was produced and followed the competition of TA–hydrazide bonds, producing an ion pair with SiO^- groups. Therefore, the anionic drug molecules lose the attraction from TA groups at pH 7–8, the highly negative surfaces of hydrolyzed and de-protonated MSN pump the anionic drug out, rapidly (Fig. 1d). Although, sulfasalazine has partly released in the duodenum pH values (5.5–6.5), the prodrug (sulfasalazine) can only be activated by a bacteria-catalyzed reaction in the colon. Thus, our design can increase the specific activation and accumulation of drug molecules in the colon. Our previous studies have shown that the modification of *N*-trimethoxysilylpropyl-*N*,*N*,*N*-trimethylammonium groups in MSN surfaces (the TA groups cannot be hydrolyzed in the stomach's pH) can increase the positive charges of MSN surfaces and, thus, an increase of loading amounts of anionic drugs can be achieved.[37] However, the further release of the adsorbed drug is also suppressed by the strong electrostatic attractions from the surface TA groups. This system exhibited sustained release for long periods (more than 20 h) and usually 10–20% of the loading drugs remained in support, finally. The residual drug molecules may be produced by an ion pair with the TA group of MSN; therefore, the adsorbed drug molecules could not achieve the overall release. For our new approach, we designed the MSN–hydrazone–TA nanocarrier through a pH-sensitive hydrazone bond, which can efficiently solve slow and incomplete release of anionic molecules in the colon's pH owing to the advanced hydrolysis of TA groups in the stomach. Finally, the cytotoxicity of MSN–hydrazone–TA was evaluated by MTT assay in the HT-29 colon cell line (Fig. 7). The HT-29 cells were treated with the MSN–hydrazone–TA sample at various concentrations (1, 2, 10, 20, 100, 200, 250, and 500 μg mL^{-1}) for 24 h. Cells without added nanoparticles were taken as the control experiment and the viability was set as 100%. The insignificant toxicity was observed in HT-29 cells even if an extremely high concentration (500 μg mL^{-1}) of MSN–hydrazone–TA was used in our MTT assay. Therefore, we can confirm that the use of MSN–hydrazone–TA as the drug carrier has the advantages of high loading of drug molecules and high biocompatibility, which can develop

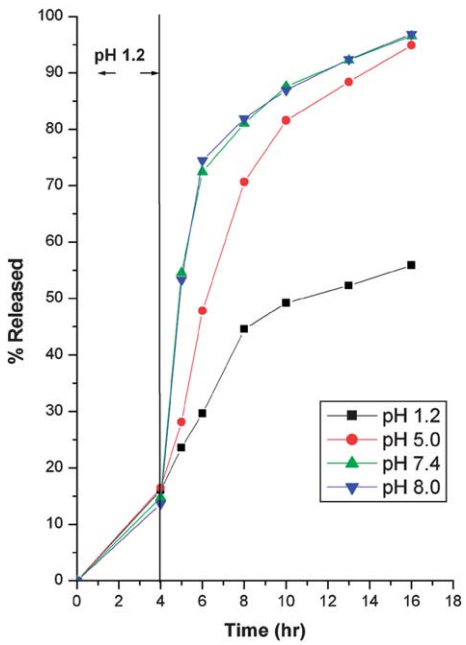

Fig. 6 Sulfasalazine released at pH 1.2 (37 °C) for 4 h, and then (▼) pH 8.0, (▲) pH 7.4, (●) pH 5.0, and (■) pH 1.2 for 16 h.

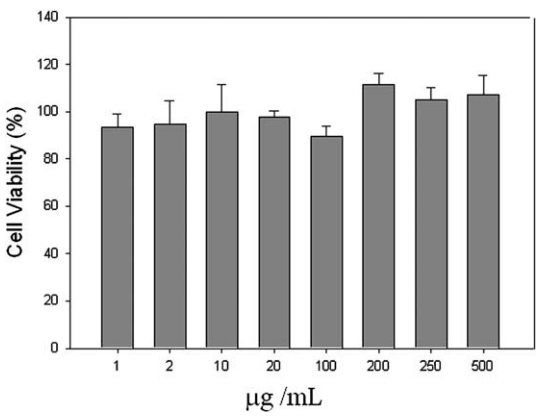

Fig. 7 MTT cytotoxicity assay of HT-29 cells treated with MSN–hydrazone–TA at various concentration ranges (1, 2, 10, 20, 100, 200, 250, 500 μg mL^{-1}) for 24 h. Cells without added nanoparticles were taken as the control experiment and the viability was set as 100%. The final report data were expressed as a percentage of the control (mean ± standard deviation).

a pH-sensitive OCDDS. The nano-sized carrier can provide both the high surface areas and the variable charges, which can increase the releasing rate in the targeted site. For our design, the targeting delivery of the therapeutic drug to the colon tissues and an enhancement of drug bioavailability can be easily achieved by increasing the release rate and the dissolution rate of a more hydrophobic drug molecule. Previously, we incorporated a high stability of the near infrared (NIR) fluorophore (Atto-647) within the MSN silica framework which provided a means of non-invasively tracking the biodistribution *in vivo*, as most mammalian tissues are relatively transparent at NIR wavelengths, and background tissue autofluorescence is minimal.[20] After oral administration of Atto-647-MSN, the nanoparticles were excreted into the feces in 12 h and therefore we observed a high fluorescent intensity in the feces. Further, the visceral groups of the dissected mouse showed that no fluorescent intensity of Atto-647-MSN revealed in the organs (Fig. S2, ESI†). Therefore, we can confirm that the MSN is mostly kept in the gastrointestinal tract and not assimilated into the systemic circulation.

Conclusion

We propose a new pH-sensitive OCDDS using MSN–hydrazone–TA nanoparticles as a drug carrier. The pH-sensitive and positively charged TA groups regulated the adsorption of anionic drugs and eliminated the TA groups through the hydrolysis of hydrazone bonds, giving the adsorbed drugs rapid and complete release. For the immobilization of various sizes of drug molecules, the pore size of MSN can be easily adjusted by directing agents that change the structure or by introduction of a swelling agent to expand the inner micelle space.[60,61] The various spectroscopic characterizations and cell viability assay indicated that the nano-sized MSN–hydrazone–TA sample exhibited both high surface areas and high biocompatibility, showing no cytotoxicity even with the treatment to the colon cell line in an extremely high nanoparticle concentration. Therefore, the self-adjusted drug release system, which has the advantages of being time dependent, pH-sensitive, and with prodrug delivery strategies, can accurately deliver the therapeutic drugs to the targeted tissue (colon). In the stomach pH, we observed only 15% release from MSN–hydrazone–TA during 4 h of gastric emptying times. Regarding the drug carriers into the stimulated environment of the colon (pH 7–8), the rapid release could be observed (80% during another 4 h) and no drug remained in support for a long period. Consequently, this type of MSN could be designed as an OCDDS to increase the drug-loading capability, the release rate in the colon pH, and further improvement of drug bioavailability.[41]

Acknowledgements

This work was supported by a research grant from the National Science Council of Taiwan (NSC 99–2113-M-259-006-MY2).

References

1 L. Yang, J. S. Chu and J. A. Fix, *Int. J. Pharm.*, 2002, **235**, 1.
2 E. Fukui, N. Miyamura, K. Uemura and M. Kobayashi, *Int. J. Pharm.*, 2000, **204**, 7.
3 S. Simovic, H. Hui, Y. M. Song, A. K. Davey, T. Rades and C. A. Prestidge, *J. Controlled Release*, 2010, **143**, 367.
4 Z. Li, S. G. Zhu, K. Gan, Q. H. Zhang, Z. Y. Zeng, Y. H. Zhou, H. Y. Liu, W. Xiong, X. L. Li and G. Y. Li, *J. Nanosci. Nanotechnol.*, 2005, **5**, 1199.
5 A. Tan, S. Simovic, A. K. Davey, T. Rades, B. J. Boyd and C. A. Prestidge, *Mol. Pharmaceutics.*, 2010, **7**, 522.
6 A. I. Raafat, *J. Appl. Polym. Sci.*, 2010, **118**, 2642.
7 N. Rouge, P. Buri and E. Doelker, *Int. J. Pharm.*, 1996, **136**, 117.
8 K. Y. Win and S. S. Feng, *Biomaterials*, 2005, **26**, 2713.
9 Y. J. Wang, Y. Yan, J. W. Cui, L. Hosta-Rigau, J. K. Heath, E. C. Nice and F. Caruso, *Adv. Mater.*, 2010, **22**, 4293.
10 H. A. Meng, M. Liong, T. A. Xia, Z. X. Li, Z. X. Ji, J. I. Zink and A. E. Nel, *ACS Nano*, 2010, **4**, 4539.
11 A. Rubinstein, *Biopharm. Drug Dispos.*, 1990, **11**, 465.
12 Y. J. Jung, J. S. Lee and Y. M. Kim, *J. Pharm. Sci.*, 2000, **89**, 594.
13 L. F. A. Asghar and S. Chandran, *J. Pharm. Pharm. Sci.*, 2006, **9**, 327.
14 M. K. Chourasia and S. K. Jain, *J. Pharm. Pharm. Sci.*, 2003, **6**, 33.
15 G. T. Macfarlane, J. H. Cummings, S. Macfarlane and G. R. Gibson, *J. Appl. Bacteriol.*, 1989, **67**, 520.
16 Y. Qiu and K. Park, *Adv. Drug Delivery Rev.*, 2001, **53**, 321.
17 Y. Chen, H. R. Chen, D. P. Zeng, Y. B. Tian, F. Chen, J. W. Feng and J. L. Shi, *ACS Nano*, 2010, **4**, 6001.
18 S. H. Cheng, C. H. Lee, M. C. Chen, J. S. Souris, F. G. Tseng, C. S. Yang, C. Y. Mou, C. T. Chen and L. W. Lo, *J. Mater. Chem.*, 2010, **20**, 6149.
19 S. H. Cheng, C. H. Lee, C. S. Yang, F. G. Tseng, C. Y. Mou and L. W. Lo, *J. Mater. Chem.*, 2009, **19**, 1252.
20 C. H. Lee, S. H. Cheng, I. P. Huang, J. S. Souris, C. S. Yang, C. Y. Mou and L. W. Lo, *Angew. Chem., Int. Ed.*, 2010, **49**, 8214.
21 J. M. Rosenholm, E. Peuhu, L. T. Bate-Eya, J. E. Eriksson, C. Sahlgren and M. Linden, *Small*, 2010, **6**, 1234.
22 M. Van Speybroeck, R. Mols, R. Mellaerts, T. Do Thi, J. A. Martens, J. Van Humbeeck, P. Annaert, G. Van denMooter and P. Augustijns, *Eur. J. Pharm. Biopharm.*, 2010, **75**, 354.
23 F. Gao, P. Botella, A. Corma, J. Blesa and L. Dong, *J. Phys. Chem. B*, 2009, **113**, 1796.
24 E. J. Anglin, L. Y. Cheng, W. R. Freeman and M. J. Sailor, *Adv. Drug Delivery Rev.*, 2008, **60**, 1266.
25 V. Cauda, L. Muhlstein, B. Onida and T. Bein, *Microporous Mesoporous Mater.*, 2009, **118**, 435.
26 C. A. Aerts, E. Verraedt, A. Depla, L. Follens, L. Froyen, J. Van Humbeeck, P. Augustijns, G. Van den Mooter, R. Mellaerts and J. A. Martens, *Int. J. Pharm.*, 2010, **397**, 84.
27 J. Hirvonen, *Eur. J. Pharm. Sci.*, 2008, **34**, S21.
28 Z. M. Tao, B. Toms, J. Goodisman and T. Asefa, *ACS Nano*, 2010, **4**, 789.
29 R. Mortera, S. Fiorilli, E. Garrone, E. Verne and B. Onida, *Chem. Eng. J.*, 2010, **156**, 184.
30 M. Vallet-Regi, F. Balas and D. Arcos, *Angew. Chem., Int. Ed.*, 2007, **46**, 7548.
31 M. Vallet-Regi, A. Ramila, R. P. del Real and J. Perez-Pariente, *Chem. Mater.*, 2001, **13**, 308.
32 M. Vallet-Regi, *Chem.–Eur. J.*, 2006, **12**, 5934.
33 D. Arcos, A. Lopez-Noriega, E. Ruiz-Hernandez, O. Terasaki and M. Vallet-Regi, *Chem. Mater.*, 2009, **21**, 1000.
34 M. Manzano and M. Vallet-Regi, *J. Mater. Chem.*, 2010, **20**, 5593.
35 M. Vallet-Regi, *J. Intern. Med.*, 2010, **267**, 22.
36 J. Andersson, J. Rosenholm, S. Areva and M. Linden, *Chem. Mater.*, 2004, **16**, 4160.
37 C. H. Lee, L. W. Lo, C. Y. Mou and C. S. Yang, *Adv. Funct. Mater.*, 2008, **18**, 3283.
38 Q. J. He, J. M. Zhang, F. Chen, L. M. Guo, Z. Y. Zhu and J. L. Shi, *Biomaterials*, 2010, **31**, 7785.
39 Q. J. He, J. L. Shi, F. Chen, M. Zhu and L. X. Zhang, *Biomaterials*, 2010, **31**, 3335.
40 I. I. Slowing, J. L. Vivero-Escoto, C. W. Wu and V. S. Y. Lin, *Adv. Drug Delivery Rev.*, 2008, **60**, 1278.
41 S. P. Rigby, M. Fairhead and C. F. van der Walle, *Curr. Pharm. Des.*, 2008, **14**, 1821.
42 C. Charnay, S. Begu, C. Tourne-Peteilh, L. Nicole, D. A. Lerner and J. M. Devoisselle, *Eur. J. Pharm. Biopharm.*, 2004, **57**, 533.
43 S. S. Huang, Y. Fan, Z. Y. Cheng, D. Y. Kong, P. P. Yang, Z. W. Quan, C. M. Zhang and J. Lin, *J. Phys. Chem. C*, 2009, **113**, 1775.

44 M. Liong, J. Lu, M. Kovochich, T. Xia, S. G. Ruehm, A. E. Nel, F. Tamanoi and J. I. Zink, *ACS Nano*, 2008, **2**, 889.
45 W. J. Xu, Q. Gao, Y. Xu, D. Wu and Y. H. Sun, *Mater. Res. Bull.*, 2009, **44**, 606.
46 Q. Gao, Y. Xu, D. Wu, Y. H. Sun and X. A. Li, *J. Phys. Chem. C*, 2009, **113**, 12753.
47 E. Aznar, M. D. Marcos, R. Martinez-Manez, F. Sancenon, J. Soto, P. Amoros and C. Guillem, *J. Am. Chem. Soc.*, 2009, **131**, 6833.
48 Y. F. Zhu, T. Ikoma, N. Hanagata and S. Kaskel, *Small*, 2010, **6**, 471.
49 S. L. Gai, P. P. Yang, C. X. Li, W. X. Wang, Y. L. Dai, N. Niu and J. Lin, *Adv. Funct. Mater.*, 2010, **20**, 1166.
50 A. Bernardos, L. Mondragon, E. Aznar, M. D. Marcos, R. Martinez-Manez, F. Sancenon, J. Soto, J. M. Barat, E. Perez-Paya, C. Guillem and P. Amoros, *ACS Nano*, 2010, **4**, 6353.
51 A. Bernardos, E. Aznar, M. D. Marcos, R. Martinez-Manez, F. Sancenon, J. Soto, J. M. Barat and P. Amoros, *Angew. Chem., Int. Ed.*, 2009, **48**, 5884.
52 A. Corma, U. Diaz, M. Arrrica, E. Fernandez and I. Ortega, *Angew. Chem., Int. Ed.*, 2009, **48**, 6247.
53 E. C. Wu, J. H. Park, J. Park, E. Segal, F. Cunin and M. J. Sailor, *ACS Nano*, 2008, **2**, 2401.
54 H. Ritter and D. Bruhwiler, *J. Phys. Chem. C*, 2009, **113**, 10667.
55 M. Kruk, M. Jaroniec, R. Ryoo and J. M. Kim, *Microporous Mater.*, 1997, **12**, 93.
56 *Nanoparticulate Drug Delivery Systems*, ed. D. Thassu, M. Deleers and Y. Pathak, 2007.
57 Y. S. Lin, C. P. Tsai, H. Y. Huang, C. T. Kuo, Y. Hung, D. M. Huang, Y. C. Chen and C. Y. Mou, *Chem. Mater.*, 2005, **17**, 4570.
58 D. L. Pavia, G. M. Lampman, G. S. Kriz, *Introduction to Spectroscopy*, 3rd edn, 2001.
59 Paul M. Dewick, *Essentials of Organic Chemistry: For Students of Pharmacy, Medicinal Chemistry and Biological Chemistry*, 1st edn, 2006.
60 J. Fan, C. Z. Yu, L. M. Wang, B. Tu, D. Y. Zhao, Y. Sakamoto and O. Terasaki, *J. Am. Chem. Soc.*, 2001, **123**, 12113.
61 D. Y. Zhao, Q. S. Huo, J. L. Feng, B. F. Chmelka and G. D. Stucky, *J. Am. Chem. Soc.*, 1998, **120**, 6024.